Deformation T-Cup: A new multi-anvil apparatus for controlled strain-rate deformation experiments at pressures above 18 GPa

Simon A. Hunt,[1,a)] Donald J. Weidner,[2] Richard J. McCormack,[1] Matthew L. Whitaker,[2] Edward Bailey,[1] Li Li,[2] Michael T. Vaughan,[2] and David P. Dobson[1]
[1]*Department of Earth Sciences, University College London, Gower Street, London WC1E 6BT, United Kingdom*
[2]*Mineral Physics Institute, Stony Brook University, Stony Brook, New York 11794-2100, USA*

(Received 5 November 2013; accepted 15 July 2014; published online 4 August 2014)

A new multi-anvil deformation apparatus, based on the widely used 6-8 split-cylinder, geometry, has been developed which is capable of deformation experiments at pressures in excess of 18 GPa at room temperature. In 6-8 (Kawai-type) devices eight cubic anvils are used to compress the sample assembly. In our new apparatus two of the eight cubes which sit along the split-cylinder axis have been replaced by hexagonal cross section anvils. Combining these anvils hexagonal-anvils with secondary differential actuators incorporated into the load frame, for the first time, enables the 6-8 multi-anvil apparatus to be used for controlled strain-rate deformation experiments to high strains. Testing of the design, both with and without synchrotron-X-rays, has demonstrated the Deformation T-Cup (DT-Cup) is capable of deforming 1–2 mm long samples to over 55% strain at high temperatures and pressures. To date the apparatus has been calibrated to, and deformed at, 18.8 GPa and deformation experiments performed in conjunction with synchrotron X-rays at confining pressures up to 10 GPa at 800 °C . [http://dx.doi.org/10.1063/1.4891338]

I. INTRODUCTION

Quantitative material property measurements at high pressures and temperatures are of interest in physics and chemistry as well as in the Earth, planetary, and materials sciences. Determination of the mineralogy deep within the Earth, as well as understanding of mineral compressibilites, the effects of pressure, temperature, and chemistry on phase transitions, and so forth have all come from using hydrostatic pressure as a tool to create extreme conditions. Pressure is an important state variable because more extreme changes in physical properties can be achieved using pressure than temperature: for many materials thermal expansion to the melting temperature does not exceed 10%, while compressions of 50% or more are possible. Dynamic properties such as rheology cannot, however, be measured under static conditions prompting recent efforts to develop techniques which are capable of making these measurements under extreme conditions. Apparatus capable of controlled deformation under extreme conditions allows high-pressure phases to be subject to dynamic property measurements under conditions of their thermodynamic stability.

The confinement of samples, in solid media devices, to significant pressures has been possible since the ground breaking work of Bridgeman in the early 20th century.[1] With his apparatus Bridgeman performed experiments at pressures up to about 10 GPa. The subsequent development of the diamond-anvil cell[45] increased the pressure range over which experiments could be performed. Early attempts to deform samples at high pressure were conducted using the diamond cell as a deformation device;[23] a technique which is still used at very high pressures.[31] More recently, hard pistons were added to nominally hydrostatic multi-anvil assemblies[3,17] to exert a differential stress onto a sample and deform it to shear strains ∼1. Both these approaches have the limitations of: (1) low total strain achievable, (2) increases in strain are convolved with increasing pressure, and (3) inability to control the timing of strain in the pressure-temperature-time path of the experiment. However, suitably designed static devices can be used with high energy X-rays or neutrons to measure processes active during deformation at high pressure in stress-relaxation experiments.[5,12,13,28] The strain-rate in stress-relaxation experiments is not constant, making the assumption of steady-state that is implicit in quantifying the data difficult to justify and the data more difficult to interpret.

A significant step in overcoming these limitations came with the development of the Deformation-DIA.[7,44] The key innovation in the D-DIA is the addition of secondary actuators within the DIA tooling which enables two of the anvils compressing the cubic sample assemblage to be advanced independently of the other four. This allows deformation to be decoupled from pressure generation. In the decade since its development the original D-DIA design has become a work-horse apparatus for controlled strain-rate deformation experiments, up to pressures around 10 GPa (around 330 km depth in the Earth) and temperatures regularly above 1500 °C. Larger versions of the D-DIA (e.g., MADONNA-1500 in Japan) or cubic presses with 6 independent actuators,[30] using the "MA6-6" anvil assembly,[34] have been used to successfully increase the pressure range of cubic presses to 25 GPa in hydrostatic experiments[20] (∼720 km depth in the Earth) and ∼20 GPa (∼575 km) in deformation experiments.[22] The D-DIA was explicitly designed to be used with synchrotron X-radiography and X-ray diffraction, which enables direct

a)Electronic mail: simon.hunt@ucl.ac.uk

measurement of the bulk and elastic strains the sample experiences during the experiment.[12,15,27,28,37] From these data, the strain-rate and stresses can be calculated which are used subsequently to determine flow-laws, anelasticity, and other dynamic properties of the sample. The D-DIA is not restricted solely to use with synchrotron X-rays. For example, Walte *et al.*[43] looked at the distribution of melts in deformed polycrystalline olivine in recovered samples and Howell *et al.*[10] investigated the textures developed during plastic deformation of diamond.

High-pressure controlled-deformation experiments have also been reported in opposed-anvil rotational devices.[2,46] In this style of device one of the anvils is rotated relative to an opposed stationary anvil, the sample is sheared between them and large strains imparted to the sample. However, they suffer from the significant drawback that their operation and interpretation of the results are more complex than those of the D-DIA and 6-axis devices. Nevertheless, results from deformation experiments in the Rotational-Drickamer Apparatus (RDA) at pressures up to 20 GPa have been reported.[16,21]

Greater hydrostatic pressures can be generated using Kawai-type apparatus[19] than in DIA type devices. Variations on the original Kawai-type design[35,41,42] have made this style of apparatus more user-friendly and the most common multi-anvil apparatus in use today. With their octahedral sample assembly, these devices are capable of generating pressures up to around 25 GPa with Tungsten Carbide anvils and to pressures in significantly above 35 GPa using sintered diamond anvils.[18,40] Despite this success, the Kawai-type apparatus has not previously been modified into a device capable of controlled strain-rate deformation experiments. Here, we report a new variation of the Kawai-type geometry, the Deformation T-Cup, which has been modified to facilitate controlled strain-rate deformation experiments.

II. THE DESIGN

The Deformation T-Cup (DT-Cup) apparatus is a development of the T-Cup design[25,26,41] (Figure 1). The T-Cup itself is a miniaturised Kawai-style apparatus, specifically designed for use with synchrotron X-rays and without any active deformation capability. It has a first stage of six hardened steel wedges, cut from a cylindrical volume. When placed together these first stage anvils form a central cubic cavity (edge length 19.5 mm) with the [111] direction of the cavity aligned along the cylinder axis, which is also the compression axis of the press (Figure 1). This first stage compresses eight 10 mm second-stage cubic anvils. These second stage anvils each have a truncation on their inner-most corner, defining an octahedral volume which contains the sample assembly. This sample assembly is larger than the octahedral void created by the anvil truncations thus the force applied to the first stage wedges is transferred to the assembly and high pressures are generated. Pyrophyllite gasketing is used to contain the sample assembly and improve cell stability at high pressure, although this comes at a cost of reduced pressure generation. The cubic inner anvils are generally made from X-ray opaque tungsten carbide (WC) anvils. Alternatively, X-ray transparent cubic boron nitride (CBN), sintered diamond,[24] or, more recently, slotted tungsten carbide anvils[4] are used, in conjunction with synchrotron X-rays, to enable radiographic imaging and the capture of full powder diffraction rings. The parts of the gasketing and pressure medium in the beam path, upstream and down-stream of the sample, can be replaced with boron epoxy windows in order to remove unwanted diffraction peaks arising from the gaskets and pressure medium.[33]

In the DT-Cup, the deformation capabilities come from redesigning the anvils oriented along the compression axis of the press ("top" and "bottom" anvils in Figure 1). The new axial anvils are cubes which have been extended along the [111] axis away from the truncated, inner, corner to make *"hexagonal anvils"* (Figure 2). The first-stage wedges are modified to create a hexagonal hole to accommodate the modified anvils (Figure 3(a)) while the confining rings are unmodified from the T-Cup. In the absence of deformation, the hexagonal anvils occupy the same volume in the wedges as the cubic anvils they replace and the modified design behaves identically to the original T-Cup design. The redesigned tooling is hosted in a modified 4.06 MN, V7, Paris-Edinburgh load frame (Figure 3(b); for a general description of the V7 load frame, see, Le Godec *et al.*[25,26]). The 150 mm diameter main piston and the breech of the press are altered to hold the 50 mm diameter secondary actuators which back the hexagonal anvils and are used for deformation. These secondary actuators are limited to a maximum of 3.1 kbar by the external plumbing and are able to exert a maximum force of 0.61 MN. The main piston and the two differential pistons are connected

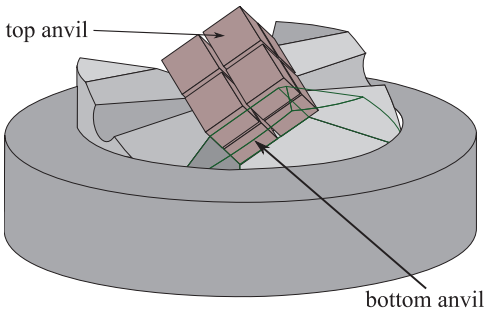

FIG. 1. The anvils, bottom wedges, and confining ring of the original T-Cup design.[41]

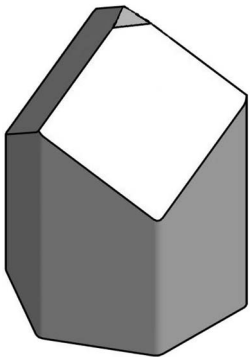

FIG. 2. Cartoon of a hexagonal anvil which enables deformation in the DT-Cup.

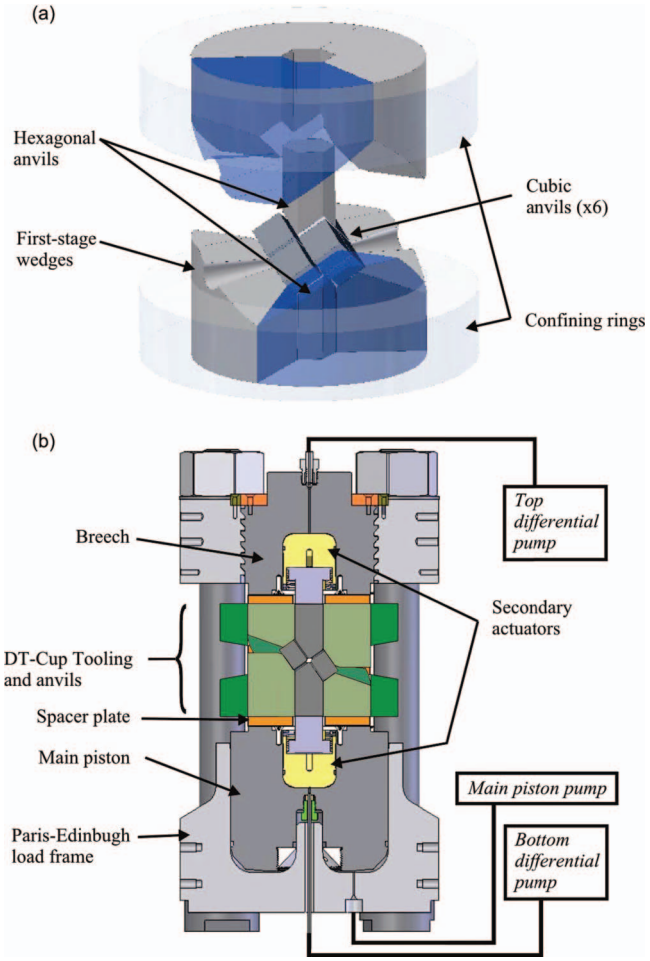

FIG. 3. Illustrations of (a) DT-Cup tooling and (b) modified Paris-Edinburgh press which holds it.

to three separate hydraulic pumps, which are independently controlled (Figure 3(b)).

Samples are heated by passing an electrical current between the wedges via the hexagonal anvils and assembly which contains a resistance furnace (e.g., Figure 4(b)). The hole in which the hexagonal anvils sit is a clearance hole and at high loads the wedges dilate sufficiently to break any electrical connection between the wedges and the hexagonal anvil. Heating of the assembly is therefore enabled by shorting the outside ends of the hexagonal pistons to spacer plates which the wedges sit on with copper braid. Thin sheets of plastic between the spacer plates and press as well as behind the hexagonal anvils insulate both sets of wedges and the hexagonal anvils from the press frame.

Two DT-Cup presses have been built, with minor differences between them. One has been deployed on X17B2ss, the monochromatic side-station beam-line to X17B2 at the NSLS, Brookhaven National Laboratory, NY and the other is at University College London (UCL). The DT-Cup at X17B2ss uses the same 10 mm cubic anvils used in the original T-Cup and hexagonal anvils that are 14.13 mm ($10 \times \sqrt{2}$) across the face-to-face diagonal of the hexagonal shank. The cubic void in the first stage wedges has a 19 mm edge length. No displacement transducers have been fitted to the apparatus because X-radiography is used to monitor the displacement of the differential pistons. The UCL DT-Cup uses larger 16 mm cubic anvils, hexagonal anvils that are 22.71 mm across the face-to-face diagonal and displacement transducers have been fitted to monitor displacement of the differential actuators. The larger anvils require a larger void in the first stage wedges, which in the UCL DT-Cup has an edge length of 29.5 mm.

The changes to the Kawai geometry, discussed here, are analogous to the modifications made to the DIA by Durham *et al.*[7] and Wang *et al.*[44] in building the D-DIA. As with the T-Cup and the D-DIA, the DT-Cup is designed to be used in conjunction with synchrotron X-rays thus enabling direct monitoring of the strain and stress in the sample during an experiment.

III. TESTING

Both DT-Cups have been successfully calibrated and tested. Synchrotron based deformation experiments have been performed at pressure up to 10 GPa, at the NSLS' monochromatic beam-line X17B2ss and offline deformation experiments have been performed at the pressures of the insulator–metal phase changes in ZnS (15.5 GPa) and GaAs (18.8 GPa).[36] A summary of the experiments discussed herein is presented in Table I. In the testing to date, the rate of anvil failure is approximately the same as that in the T-Cup or any other multi-anvil using small sized cubes and the cell design

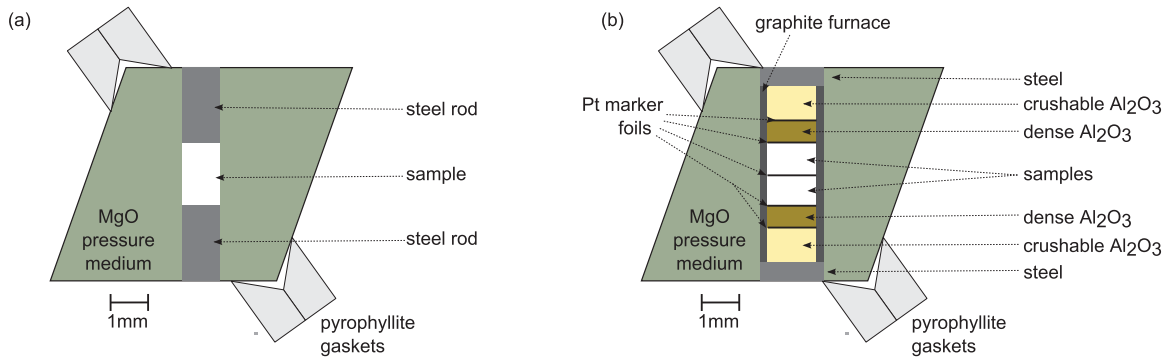

FIG. 4. Cross-section through sample assemblies and gasketing used in the (a) offline electrical resistance calibrations and (b) online X17B2ss tests. For clarity the thermocouple, which comes in from the side, has been omitted from (b).

TABLE I. The summary of the cell designs and conditions of experiments discussed herein. The cell designs refereed to in the table are presented in Figure 4. The pressures during deformation are approximate. See Figure 9 for how the pressure changes with strain.

Experiment	Location	Sample	Force (kN)	Temperature (°C)	Pressure		Deformation[a] [strain (%) or shortening (μm)]	Expt. type and assembly design
					Before annealing (GPa)	During deformation (GPa)		
DT14-004	UCL (offline)	ZnS	1120	25	15.5	15.5	463 μm	Resistance (Fig. 4(a))
DT14-002	UCL	GaAs	1435	25	18.8	18.8	214 μm	Resistance
SiO_38	X17B2ss (online)	SiO_2 + olivine	390	800	8.8	~2	~53%	X-ray, no Al_2O_3 sleeve (Fig. 4(b))
SiO_39	X17B2ss	SiO_2 + olivine	946	800	14.2	~9.5	~6%	X-ray, no Al_2O_3 sleeve
SiO_40	X17B2ss	Quartz + olivine	113	800	3.3	~3	~56%	X-ray, no Al_2O_3 sleeve
SiO_43	X17B2ss	SiO_2 + olivine	445	800–1300	9.0	~7	~32%	X-ray, inc. Al_2O_3 sleeve and boron epoxy windows
Fe_15	X17B2ss	Fe	951	500	12.5		Not deformed	X-ray, inc. Al_2O_3 sleeve and boron epoxy windows

[a]Deformation is presented as strain for X17B2ss experiments and shortening for offline experiments because of how the deformation is measured in the experiments.

presented here is highly robust to blow-outs, with only one experienced so far in over 20 experiments.

In all the experiments, the behaviour of the two independent differential pistons is very similar and the pressures in each differential actuator track each other closely. In the following discussion, therefore, the differential systems are presented as a single system although there are really two systems performing identical actions. The differential oil pressure presented is the mean of the pressures in the top and bottom pistons, the differential oil volume is the sum of the oil volume displaced by the pumps and the oil flow rate is the time derivative of this. The displacement of the differential anvils is the combined displacement of both the top and bottom anvils.

A. Sample assemblies and anvils

The sample assemblies used in the DT-Cup commissioning experiments (Figure 4) are similar to those used in traditional Kawai-type apparatus. Each assembly consisted of a 7 mm edge-length, MgO, octahedral pressure medium which was compressed by anvils with 3 mm truncations; generally referred to as a 7/3 assembly. In the ZnS and GaAs experiments the samples were mounted directly in the MgO pressure medium and electrically connected to the axial anvils by 2 mm long, 1 mm diameter steel rods (Figure 4(a)). For the X17B2ss experiments, a 4.7 mm long, straight-cylindrical graphite furnace with a 1.2 mm internal diameter and 200 μm wall thickness was surrounded by the pressure medium; 0.5 mm thick steel disks on the ends of the furnace provided electrical contact with the anvils and prevented the graphite from coming into direct contact with the hexagonal anvils (Figure 4(b)). Some experiments had additional, 1 mm wall thickness, sleeves of crushable alumina between the furnace and the MgO pressure medium; this substantially improved the pressure and temperature efficiency (see Sec. III C). Each experiment had a sample composed of two cylinders, approximately 0.8 mm long, of compressed powders: one of San Carlos olivine and the other of silica. In the present experiments the silica sample was loaded as amorphous SiO_2, except for the lowest pressure experiment in which a quartz sample was used instead. These two samples were sandwiched between two 0.6 mm long corundum pistons and each of these 4 pieces was separated from each other by 25 μm Platinum foil disks. A thermocouple was inserted through the side of the octahedron to butt up against the outside of the furnace but not making electrical contact. The assembly is oriented in the press with the furnace running between the two hexagonal anvils and aligned with the axis of the press.

For the experiments discussed here, 2 × 2 mm cross-section gaskets with a right-angled V-shaped slot cut in the front to accommodate the corners of the octahedral assembly were used (Figure 4). Boron epoxy windows through the gaskets were used in some experiments to improve the quality of the diffraction patterns and test their effect on the gaskets during deformation. Fibre glass or mica sheets are used between the cubic and the first-stage anvils as is normal in Kawai-style apparatus. In the offline experiments all WC anvils were used but in the online experiments 2 × WC hexagonal anvils, 2 × WC cubic anvils, and 4 × CBN cubic anvils were used; using 4 X-ray transparent CBN anvils is sufficient to enable imaging of the entire sample.[11]

B. Experimental protocol

The same basic procedure is adopted for all the experiments discussed here. The assembly is compressed, over a few hours, to the desired end-load with the differential actuators fully retracted. After heating and annealing of the sample, the differential oil pumps are advanced rapidly until the differential pistons are lifted from their retracted positions. The point at which the pistons lift is monitored using X-radiographic imaging at the X17B2ss and displacement transducers at UCL. The sample is then deformed at the desired rate by slowly advancing the differential oil pumps until the desired total strain in the sample is achieved or the desired time has elapsed. Multiple strain-rate or temperature steps can be performed in the same experiment by changing the oil flow rate in the differential pumps or the power applied to the furnace. When the desired total sample strain is reached the dif-

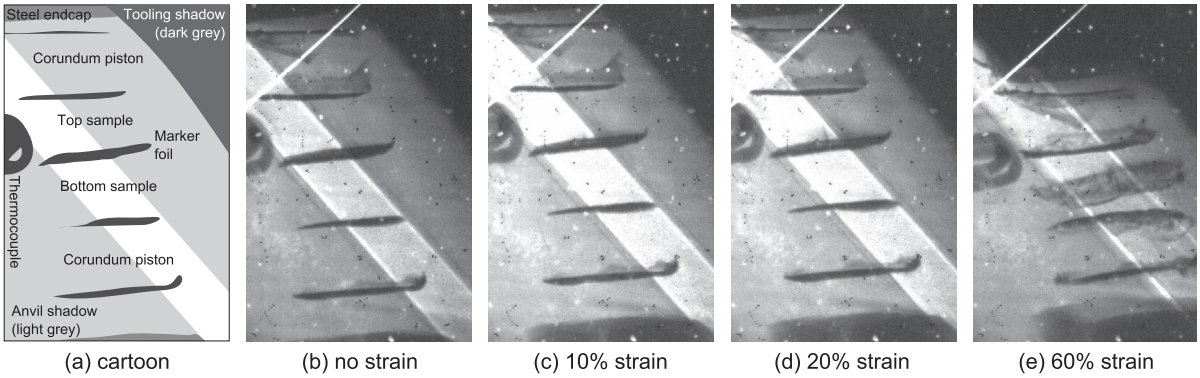

FIG. 5. X-radiographs. Drawing illustrating features typically seen in radiography images (left) and radiography images of the sample with no strain (second from left) through to 60% strain (right) from deformation experiment SiO_38. Part (e) is included to demonstrate the deformation to large strains is possible. The bright stripe going from top left to bottom right in the image is the gap between the anvils, which increases in width with increasing strain. The bright white line along the top left of each image is from a crack in the phosphorescent YAG crystal used in the imaging.

ferential pumps are stopped, the experiment is quenched and the assembly is decompressed, usually over more than 5 h to preserve the anvils. If recovery of the sample is important the positions of the differential pistons are held constant during decompression by retracting the differential pumps at the rate required to hold the pistons. If the sample does not need to be recovered the differential pumps are retracted to their initial position and then main load removed.

During deformation, the end load on the press is maintained, at a constant value, by bleeding hydraulic oil from the main ram. In response to the differential force and the advance of the differential anvils, the main ram retreats fractionally allowing the cubic side anvils to dilate. The dilation of the cubic anvils is constrained by the geometry of the system.

Throughout the ZnS and GaAs experiments the electrical resistance across the samples was measured. These two semiconductors undergo insulator–metal transitions at 15.5 GPa and 18.8 GPa, respectively,[36] during which the electrical resistance drops over the course of a few kilonewton increase in confining force from greater than 10^4 Ω to less than 1 Ω. The transition pressure is taken as point at which the resistance starts its rapid decrease. In order to asses any changes in pressure during deformation, compression of the assembly was stopped approximately half-way between the "insulator" and "metal" resistance values and held at this value while the samples were deformed. Before the experiment was decompressed, the differential pumps were driven backwards, retracting the pistons, to their initial positions. No heating or annealing steps were performed during these experiments.

For the X17B2ss experiments, following compression the sample was annealed at 800 °C for between 2 and 4 h before deformation. Deformation was carried out at up to three separate differential oil flow rates in each experiment at constant temperature or the temperature was increased step wise at constant differential oil flow rate. During the deformation stage of the experiments X-radiographs were acquired and towards the end of each stage of the experiment X-ray diffraction patterns were acquired from each of the samples and one of the corundum pistons. The radiographic images were collected using a visible light camera and a fluorescent Ytrrium-Aluminium Garnet crystal with an exposure of 5 s at a rate of 1 per minute. Example images from the one of the experiments are shown in Figure 5. The change in position of the marker foils between each image was tracked using a pixel cross-correlation method[12,28] from which the sample strains and strain rates were calculated. The strain and strain-rates referred to in the subsequent discussion are calculated from the combined length of both the San Carlos and silica samples. By taking ratios of the strain-rate in the silica polymorphs to that of olivine the relative strengths of SiO_2-polymorphs can be constrained; we will present these results in a separate paper.

Diffraction patterns were captured on a MAR345 image plate with an exposure time of 300 s. The energy of the monochromatic X-ray beam and the MAR image plate parameters for all the experiments were determined from ceria (CeO_2) diffraction patterns taken before the experiments started and analysed in Fit2D.[8,9] Diffraction patterns from the experiments with boron-epoxy windows in the gaskets were very clean (Figure 6) with diffraction peaks clearly visible and indexable. In the experiments without boron-epoxy gasket windows, however, diffraction from the pyrophyllite gaskets and MgO pressure medium obscured the sample diffraction peaks and it was not possible to reliably calculate pressure or differential stresses from the olivine samples. In all the experiments though unique diffraction peaks from corundum were identifiable and used to determine the pressure from the equation of state of Dubrovinsky *et al.*[6] In the 946 kN experiment, which did not use boron-epoxy windows, diffraction peaks from stishovite were also distinct and the pressure was determined from the unit cell volumes using the equation of state of Nishihara *et al.*[32]

The temperatures used in calculating the pressures were those measured by the thermocouple even though the temperature in the corundum or sample is unlikely to be the same as that measured by the thermocouple. The external thermocouple measures significantly lower temperatures than those experienced by sample[14] and at high temperatures there are significant thermal gradients along the furnace axis.[38] The temperature difference between the diffraction volumes and the thermocouple has not been calibrated and therefore the temperature used in calculating the pressure is that of the

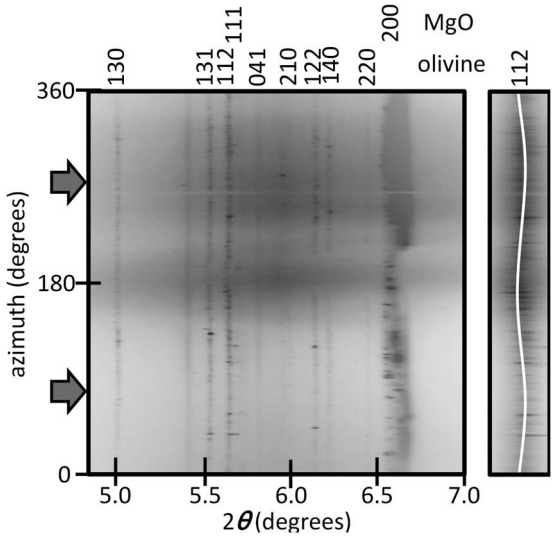

FIG. 6. Sample olivine diffraction pattern from experiment SiO_43 (445 kN) during deformation at 800 °C. The diffraction pattern has been unwrapped to allow distortions of the Debye rings to be recognised. The vertical axis is the angle of the diffraction vector from horizontal (0°). The grey arrows at 90° and 270° denote the orientation of the maximum stress direction, which are vertical in the press; the differential stress was measured to be 1.0 ± 0.3 GPa. Despite the boron epoxy windows significantly improving the pattern, there are still diffraction peaks from MgO, graphite, and crushable alumina present in the diffraction pattern. The doubling of the MgO {200} peak arises because the MgO is up-stream and down-stream of the sample making two different volumes with different "sample"–detector distances; the unindexed diffraction peaks are from the graphite heater and crushable alumina insulating sleeve. On the right-hand side the sub-figure expands {112} olivine diffraction peak and highlights its modulations due to the applied stress.

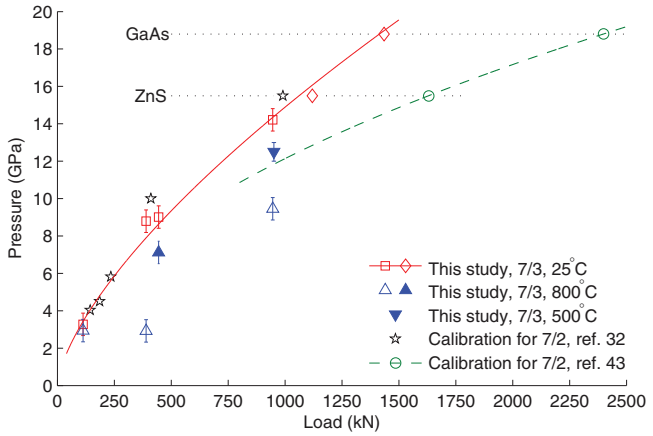

FIG. 7. Pressure calibrations for the 7/3 assembly with the 2 mm deep gaskets (see text for details) before deformation was started. The open and filled triangular symbols denote, respectively, the experiments without and with crushable alumina insulating sleeves.

thermocouple. If it possible therefore that calculated pressures are an overestimate of the actual pressure but this can only be a small amount or the stable phase of SiO_2 would be different.

C. Pressure calibration

The pressure generating capabilities of the DT-cup were tested using both the semiconductor phase transitions and X-ray diffraction from the samples and are plotted in Figure 7. The assembly used here is very efficient at generating high pressure at ambient temperatures. Our assembly is significantly more effective than the 7/2 assembly (a 7 mm octahedron compressed by anvils with 2 mm corner) used previously by Liebermann and Wang[29] (◯, Figure 7). Le Godec *et al.*[25] used T-Cup tooling in a V7 Paris-Edinburgh load frame to calibrate their 7/2 assembly (☆, Figure 7), which is very close in pressure generating capabilities to the 7/3 used in this study. Theoretically, a 7/2 assembly should be more pressure efficient than a 7/3 assembly for the same load[39] but the volume of gasketing present has a significant effect on the pressure generation. Here, we have used much less gasketing than was used in the studies mentioned above. The pressure calibration for the DT-Cup using standard 8/3 assemblies and gaskets is very similar to the calibration of the same assembly in a Walker-type multi-anvil.

After annealing at 800 °C, diffraction patterns from the SiO_2 samples in the experiments at 113, 390, 445 and 946 kN (SiO_40, 38, 43, 40, respectively, Table I) show that they were quartz, coesite, coesite, and stishovite. The quartz and coesite patterns were not clean enough for the pressure to be calculated from them but it was possible to calculate the pressure from the stishovite sample which gave the same pressure as the corundum. Another experiment at 951 kN (Fe_15) synthesised hcp-Fe at 500 °C; no bcc or fcc-Fe peaks were observed in the diffraction patterns. The pressure in this experiment was calculated to be 12.5 GPa. In experiments SiO_38 and 39, there are significant reductions in pressure after annealing the samples at 800°C (Figure 7, △). The decrease in pressure is due to a large furnace in an assembly predominantly made from poorly-insulating MgO and the densification of the large amorphous silica sample as it transforms to stishovite or coesite. The pressure loss is significantly lower in SiO_40 because the starting sample was quartz rather than amorphous SiO_2 and in the experiments where crushable alumina insulation was added to the cell (▼, ▲ Figure 7).

D. Pressure during deformation

The deformation experiments with ZnS and GaAs samples (DT14-004 and -002, respectively) used the electrical resistance of the semiconductors as a probe of the pressure during deformation. The same systematics were observed during deformation of both samples; here the GaAs experiments are discussed and Figure 8 shows the resistance, differential forces, and oil volumes during this experiment. Compression of the assembly was stopped approximately half way between the "insulator" and "metal" resistance values at 1436 kN, when the pressure in the sample was a little above the 18.8 GPa transition pressure. At this confining force the differential pumps were advanced moving the differential actuators. During the initial rapid advancement of the differential pumps there is little movement of the differential actuators but after ∼12.5 cm^3 of oil has been displaced the differential pistons advance more rapidly. This is the point at which the differential actuators are floated and the large displacement of the differential anvils is accompanied by a reduction of the re-

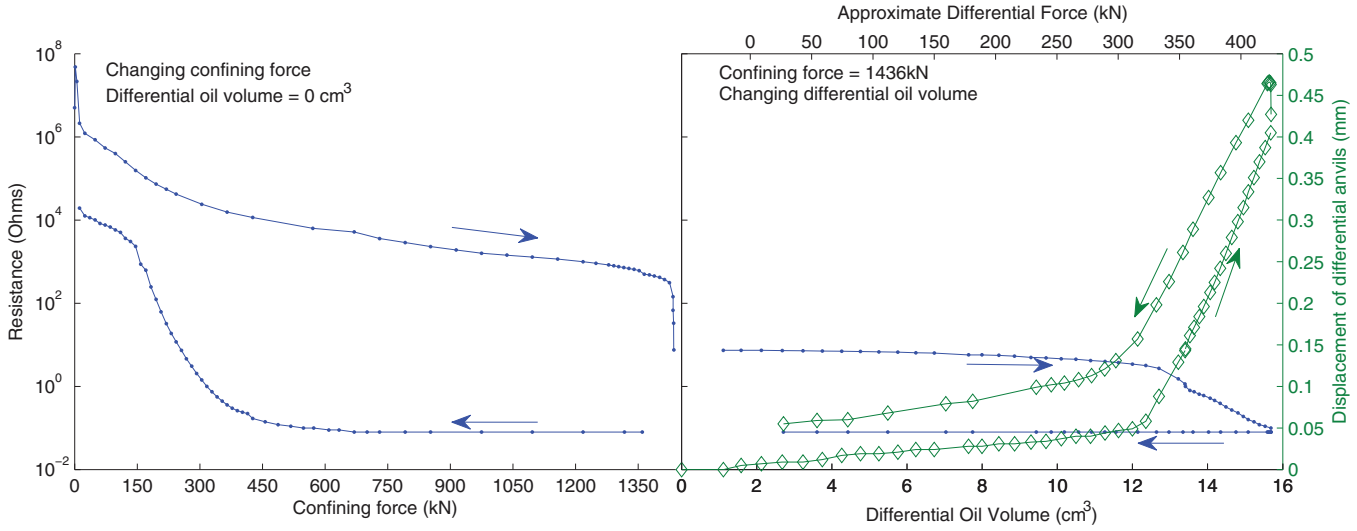

FIG. 8. Electrical resistance (dots) measured, in DT14-004, across the GaAs sample during a calibration and deformation test. The left hand side of the figure shows the resistance while the confining force is increased or decreased while the right hand side shows the resistance and differential oil volume (green, diamonds) across the cell against displacement of the differential anvils. The differential force is the mean of the force measured at that volume during advance and retraction of the differential rams.

sistance across the sample. After a total of 0.47 mm of shortening had been imparted to the assembly (∼15 % strain in the compressed octahedron) the differential pumps were retracted during which the resistance across the sample remained constant. The sample resistance only recovers to its "insulator" value during decompression at a confining force of approximately 300 kN. The decrease in resistance during decompression of the assembly demonstrates that the sample pressure did not drop significantly during deformation and the pressure during deformation was therefore above 18.8 GPa.

In the X17B2ss experiments, the displacement of the differential actuators is not measured directly but strain in the sample, calculated from the X-radiographs, is used as a proxy for displacement of the differential anvils. The strain from X-radiographs acquired immediately before and after the diffraction patterns was averaged to give the mean strain in the sample during the diffraction acquisition. The change in pressure as a function of strain can then be determined, by plotting pressure against strain (Figure 9). At constant temperature, the pressure during deformation is constant to within the spread of the data. In SiO_39 (946 kN) the calculated pressures in the stishovite and corundum are within error of each other and roughly constant at 9.2 GPa and in SiO_40 and _38 (113 and 390 kN) there is little pressure drop even at strains in excess of 50%. However, in the experiment where the temperature was increased stepwise the pressure decreases with increasing strain and temperature because there is a general thermal relaxation of the pressure medium and gaskets. There is no indication in the data of a strain-rate dependence to the pressure.

E. Press mechanics during deformation

The forces on the pistons and the temperature profile for a typical experiment are shown in Figure 10. While the deformation rams are advancing, the force exerted by the main piston is kept constant but the force exerted by the differential rams (and the differential oil pressure) increases significantly. The differential actuators are housed within the main-ram and breech of the press and act both to strain the sample and against the confining force provided by the main-ram. Balance of forces requires that the force exerted by the main ram on the non-differential cubic anvils must therefore decrease, enabling them to dilate out of the way of the differential anvils. The increase in force on the differential anvils and corresponding reduction on the cubic anvils balance out to keep the sample pressure approximately constant as a function of strain (Figure 9). In the current experiments movement of the wedges was not measured but gap between the cubic anvils can be measured from the radiography images. In experiment SiO_38 (Figure 5), the anvil gap has increased by approximately 2% at 20% strain and by ∼14% at 55% strain.

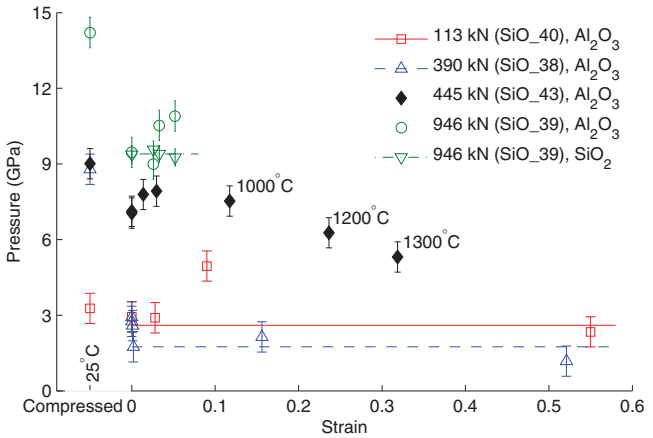

FIG. 9. Pressure as a function of strain during the experiments in this study; the forces in the legend refer to the confining force at which the experiments were performed. The "compressed" pressure is the pressure measured before heating, the pressures at zero strain are those before deformation was started. All temperatures are after compression are 800 °C unless otherwise stated. The error bars are one standard deviation.

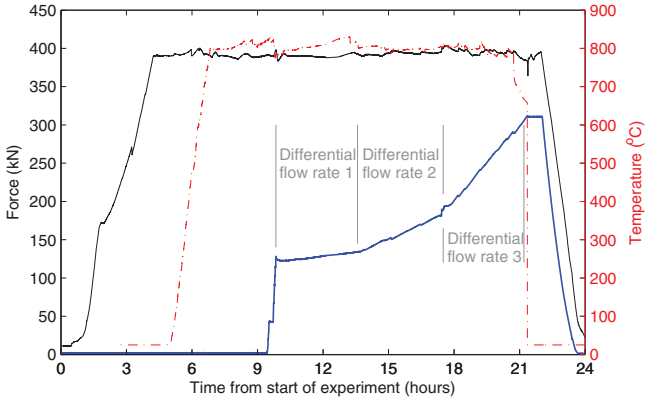

FIG. 10. Force and temperature plot for SiO_38 (390 kN). Force on main piston – black line, mean force on differential rams – blue line, temperature – dashed red line. The X-radiography images and accompanying strains from this experiment are shown in Figures 5 and 11. The noise in the force and temperature profiles is due to insensitivity in the feedback parameters of the control system.

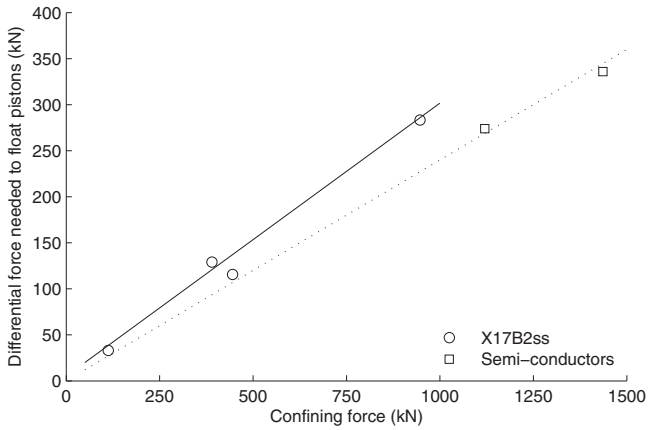

FIG. 12. Force needed to float differential anvils as a function of confining force. The circles are for the X17B2ss experiments and the squares for the semi-conductor experiments. The solid and dashed lines are the fits through the data passing through the origin.

We note here that the differential force is not a function of strain-rate but is a reproducible function of strain. This suggests that the cause is internal friction in the cell and not pressure-lag in the oil lines. This is further confirmed by the fact that when the differential pumps are stopped at high forces there are only trivial changes in the position of the pistons. If the system was over-driven it should be expected that the differential pistons continue to advance after the pumps have stopped. The behaviour of the differential system is consistent with that observed in the D-DIA, although the rate of increase in the differential force with strain appears to be much greater in the DT-Cup as would be expected since 6–8 geometries have significantly more gasketing than DIA geometries.

The total strain in the sample, used here as a proxy for the advance of the differential pistons, is a function of oil volume displaced by the differential pumps and the end load (Figure 11(a)). Higher end loads require a greater volume of oil to be displaced before the differential anvils first move and strain in the sample can be observed X-radiographically. The amount of strain per unit volume of oil decreases with increasing end load. At constant temperature, the strain-rate in the sample is an approximately linear function of oil displacement rate (Figure 11(b)) and, for a constant oil displacement rate, decreases with increasing end load. At constant differential flow rates higher temperatures correspond to faster sample strain-rates as more of the assembly-strain partitions into the hot-part of the assembly.

The volume of oil needed to initially displace the differential pistons scales with the end load (Figure 12). For the standard amount of gasketing used in the experiments here the force required to move the differential pistons is 0.30 of the confining force. The forces required to lift the differential actuators in the GaAs and ZnS experiments was ∼0.24 times the confining force. The lower value for floating the differential actuators in the semi-conductor experiments is because in

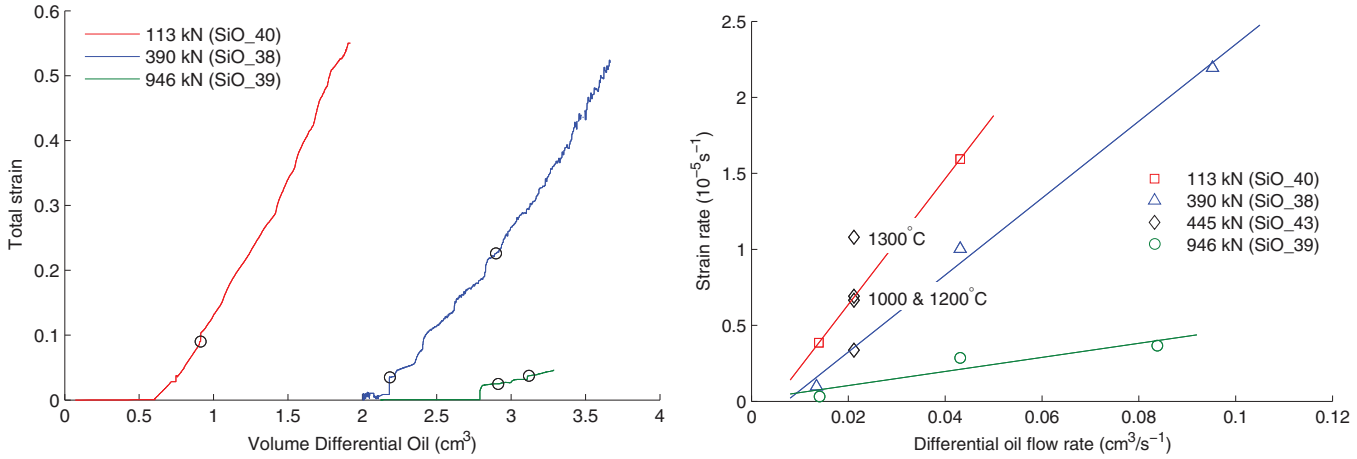

FIG. 11. Relationship between strain and differential oil volume. (a) Total strain in sample as a function of end load and oil volume moved by differential pumps. The black circles highlight the oil volumes at which the flow rate changed and the forces in the legend refer to the confining force the experiment was performed at. The data at zero strain, prior to the first motion of the differential pistons, have been omitted for clarity. (b) Strain-rate vs. oil flow rate for the same experiments and additional data from the temperature ramp experiment SiO_43. All data are at 800 °C unless otherwise annotated.

these experiments the first motion of the differential actuators can be observed directly using the displacement transducers (as in Figure 8) but in the X17B2ss experiments the actuators have to have moved a significant distance before the displacement can be observed, by eye, in the X-radiographs. Theoretically, the force required to advance the differential actuators in the octahedral geometry is a quarter of the confining force. This is consistent with the experimental values measured here and with D-DIA where the force required to move the differential pistons is approximately 1/3 of the confining-force.

IV. DISCUSSION

The results presented here demonstrate that the DT-Cup variation on the Kawai-type geometry can be used for deformation experiments in a manner similar to that which the deformation-DIA geometry has been for the past decade. It is a viable apparatus capable of performing deformation experiments at pressures above 18 GPa at modest end-loads and is reliable and reproducible in its experimental operation. The rate of experimental and anvil failures are not significantly greater than that in the T-Cup or other static Kawai devices, although the number of experiments currently performed in the DT-Cup is small.

The DT-Cup devices discussed here are limited in the volume of sample they can act on by the small size of the anvils. The pressure at which samples can be deformed is limited by the maximum force available in the differential actuators which in turn is determined by their small diameters and the maximum oil pressure of the control system. However, future developments of larger DT-Cup style machines will overcome many of the limitations of the current generation of devices.

ACKNOWLEDGMENTS

S.A.H. was funded by NERC post-doctoral research fellowship (NE/H016309/1). S.A.H. and L.L. were funded by NSF Grant No. EAR0809397. R.J.M. was funded by Marie Curie Research Training Network "c2c" Contract No. MRTN-CT-2006-035957. Neil Hughes is thanked for his technical support for the project and Figure 2. Use of the National Synchrotron Light Source, Brookhaven National Laboratory, was supported by the U.S. Department of Energy, Office of Science, Office of Basic Energy Sciences, under Contract No. DE-AC02-98CH10886. Use of the X17B2 beamline was supported by COMPRES, the Consortium for Materials Properties Research in Earth Sciences under NSF Cooperative Agreement EAR 10-43050 and by the Mineral Physics Institute, Stony Brook University.

We thank the two anonymous reviewers for their comments which resulted in a much improved paper.

[1]Bridgman, P. W., *The Physics of High Pressure* (Dover Publications, 1931).
[2]Bromiley, G., Redfern, S., Le Godec, Y., Hamel, G., and Klotz, S., "A portable high-pressure stress cell based on the V7 Paris-Edinburgh apparatus," High Pressure Res. **29**(2), 306–316 (2009).
[3]Bussod, G. Y., Katsura, T., and Rubie, D. C., "The large volume multi-anvil press as a high P-T deformation apparatus," Pure Appl. Geophys. **141**(2–4), 579 (1993).
[4]Dobson, D. P., Hunt, S. A., and Müller, H. J., "Slotted carbide anvils: improved X-ray access for synchrotron-based multi-anvil experiments," High Pressure Res. **32**(4), 532–536 (2012).
[5]Dobson, D. P., Mecklenburgh, J., Alfe, D., Wood, I. G., and Daymond, M. R., "A new belt-type apparatus for neutron-based rheological measurements at Gigapascal pressures," High Pressure Res. **25**(2), 107–118 (2005).
[6]Dubrovinsky, L. S., Saxena, S. K., and Lazor, P., "High-pressure and high-temperature *in situ* x-ray diffraction study of iron and corundum to 68 GPa using an internally heated diamond anvil cell," Phys. Chem. Miner. **25**, 434–441 (1998).
[7]Durham, W., Weidner, D., Karato, S., and Wang, Y., "New developments in deformation experiments at high pressure," in *Plastic Deformation of Minerals and Rocks*, Reviews in Mineralogy and Geochemistry, edited by S.Karato and H.Wenk (Mineralogical Society of America, 2002), pp. 21–49.
[8]Hammersley, A. P., Svensson, S. O., Hanfland, M., Fitch, A. N., and Hausermann, D., "Two-dimensional detector software: From real detector to idealised image or two-theta scan," High Pressure Res. **14**(4–6), 235–248 (1996).
[9]Hammersley, A. P., Svensson, S. O., Thompson, A., Graafsma, H., Kvick, A., and Moy, J. P., "Calibration and correction of distortions in two-dimensional detector systems," Rev. Sci. Instrum. **66**(3), 2729–2733 (1995).
[10]Howell, D., Piazolo, S., Dobson, D., Wood, I., Jones, A., Walte, N., Frost, D., Fisher, D., and Griffin, W., "Quantitative characterization of plastic deformation of single diamond crystals: A high pressure high temperature (HPHT) experimental deformation study combined with electron backscatter diffraction (EBSD)," Diamond Relat. Mater. **30**, 20–30 (2012).
[11]Hunt, S. A., Davies, D. R., Walker, A. M., McCormack, R. J., Wills, A. S., Dobson, D. P., and Li, L., "On the increase in thermal diffusivity caused by the perovskite to post-perovskite phase transition and its implications for mantle dynamics," Earth Planet. Sci. Lett. **319–320**, 96–103 (2012).
[12]Hunt, S. A., Dobson, D. P., Brodhold, J., Li, L., and Weidner, D., "Relative strength of the pyrope–majorite solid solution and the flow-law of majorite containing garnets," Phys. Earth Planet. Inter. **179**, 87–95 (2010).
[13]Hunt, S. A., Dobson, D. P., Wood, I. G., Brodhold, J., Mecklenburgh, J., and Oliver, E. C., "Deformation of olivine at 5 GPa and 350–900 °C," Phys. Earth Planet. Inter. **172**, 84–90 (2009).
[14]Hunt, S. A., Walker, A. M., McCormack, R., Dobson, D. P., Wills, A. S., and Li, L., "The effect of pressure on thermal diffusivity in pyroxenes," Mineral. Mag. **75**(5), 2597–2610 (2011).
[15]Hunt, S. A., Weidner, D. J., Li, L., Wang, L., Walte, N., Brodholt, J. P., and Dobson, D. P., "Weakening of $CaIrO_3$ during the perovskite-post perovskite transformation," Nat. Geosci. **2**, 794–797 (2009).
[16]Hustoft, J., Amulele, G., Ando, J.-i., Otsuka, K., Du, Z., Jing, Z., and Karato, S.-i., "Plastic deformation experiments to high strain on mantle transition zone minerals wadsleyite and ringwoodite in the rotational Drickamer apparatus," Earth Planet. Sci. Lett. **361**, 7–15 (2013).
[17]Karato, S. and Rubie, D. C., "Toward an experimental study of deep mantle rheology: A new multianvil sample assembly for deformation studies under high pressures and temperatures," J. Geophys. Res. **102**(B9), 20111–20122, doi:10.1029/97JB01732 (1997).
[18]Katsura, T., Yokoshi, S., Kawabe, K., Shatskiy, A., Okube, M., Fukui, H., Ito, E., Nozawa, A., and Funakoshi, K.-i., "Pressure dependence of electrical conductivity of $(Mg,Fe)SiO_3$ ilmenite," Phys. Chem. Miner. **34**(4), 249–255 (2007).
[19]Kawai, N. and Endo, S., "The generation of ultrahigh hydrostatic pressures by a split sphere apparatus," Rev. Sci. Instrum. **41**, 1178–1181 (1970).
[20]Kawazoe, T., Nishiyama, N., Nishihara, Y., and Irifune, T., "Pressure generation to 25 GPa using a cubic anvil apparatus with a multi-anvil 6-6 assembly," High Pressure Res. **30**(1), 167–174 (2010).
[21]Kawazoe, T., Karato, S.-i., Ando, J.-i., Jing, Z., Otsuka, K., and Hustoft, J. W., "Shear deformation of polycrystalline wadsleyite up to 2100 K at 1417 GPa using a rotational Drickamer apparatus (RDA)," J. Geophys. Res. **115**, B08208, doi:10.1029/2009JB007096 (2010).
[22]Kawazoe, T., Ohuchi, T., Nishiyama, N., Nishihara, Y., and Irifune, T., "Preliminary deformation experiment of ringwoodite at 20 GPa and 1700 K using a D-DIA apparatus," J. Earth Sci. **21**(5), 517–522 (2010).
[23]Kinsland, G. L. and Bassett, W. A., "Modification of the diamond cell for measuring strain and the strength of materials at pressures up to 300 kilobar," Rev. Sci. Instrum. **47**(1), 130 (1976).
[24]Kondo, T., Sawamoto, H., Yoneda, A., Kato, M., Matsumuro, A., Yagi, T., and Kikegawa, T., "The use of sintered diamond anvils in the MA8 type high-pressure apparatus," Pure Appl. Geophys. **141**(2–4), 601–611 (1993).

[25]Le Godec, Y., Hamel, G., Martinez-Garcia, D., Hammouda, T., Solozhenko, V. L., and Klotz, S., "Compact multianvil device for *in situ* studies at high pressures and temperatures," High Pressure Res. **25**(4), 243–253 (2005).
[26]Le Godec, Y., Hamel, G., Solozhenko, V. L., Martinez-Garcia, D., Philippe, J., Hammouda, T., Mezouar, M., Crichton, W. A., Morard, G., and Klotz, S., "Portable multi-anvil device for *in situ* angle-dispersive synchrotron diffraction measurements at high pressure and temperature" J. Synchrotron Radiat. **16**(4), 513–523 (2009).
[27]Li, L., Long, H., Raterron, P., and Weidner, D. J., "Plastic flow of pyrope at mantle pressure and temperature," Am. Mineral. **91**, 517–525 (2006).
[28]Li, L., Raterron, P., Weidner, D. J., and Chen, J., "Olivine flow mechanisms at 8 GPa," Phys. Earth Planet. Inter. **138**, 113–129 (2003).
[29]Liebermann, R. C. and Wang, Y., "Characterization of sample environment in a uniaxial split-sphere apparatus," *High-Pressure Research: Application to Earth and Planetary Sciences* (Terra Scientific Publishing Company, 1992), pp. 19–31.
[30]Manthilake, M. A., Walte, N., and Frost, D. J., "A new multi-anvil press employing six independently acting 8 MN hydraulic rams," High Pressure Res. **32**, 195–207 (2012).
[31]Merkel, S., McNamara, A. K., Kubo, A., Speziale, S., Miyagi, L., Meng, Y., Duffy, T. S., and Wenk, H.-R., "Deformation of (Mg,Fe)SiO_3 post-perovskite and D″ anisotropy," Science **316**(5832), 1729–1732 (2007).
[32]Nishihara, Y., Nakayama, K., Takahashi, E., Iguchi, T., and Funakoshi, K.-c., "P–V–T equation of state of stishovite to the mantle transition zone conditions," Phys. Chem. Miner. **31**, 660–670 (2005).
[33]Nishihara, Y., Tinker, D., Kawazoe, T., Xu, Y., Jing, Z., Matsukage, K. N., and Karato, S., "Plastic deformation of wadsleyite and olivine at high-pressure and high-temperature using a rotational Drickamer apparatus (RDA)," Phys. Earth Planet. Inter. **170**(3–4), 156–169 (2008).
[34]Nishiyama, N., Wang, Y., Sanehira, T., Irifune, T., and Rivers, M., "Development of the multi-anvil assembly 6-6 for DIA and D-DIA type high-pressure apparatuses," High Pressure Res. **28**(3), 307–314 (2008).
[35]Onodera, A., "Octahedral-anvil high-pressure devices," High Temp. – High Pressures **19**, 579–609 (1987).
[36]Onodera, A. and Ohtani, A., "Fixed points for pressure calibration above 100 kbars related to semiconductor-metal transitions," J. Appl. Phys. **51**(5), 2581–2585 (1980).
[37]Raterron, P., Girard, J., and Chen, J., "Activities of olivine slip systems in the upper mantle," Phys. Earth Planet. Inter. **200–201**, 105–112 (2012).
[38]Raterron, P., Merkel, S., and Holyoke, C. W., "Axial temperature gradient and stress measurements in the deformation-DIA cell using alumina pistons," Rev. Sci. Instrum. **84**(4), 043906 (2013).
[39]Shatskiy, A., Katsura, T., Litasov, K., Shcherbakova, A., Borzdov, Y., Yamazaki, D., Yoneda, A., Ohtani, E., and Ito, E., "High pressure generation using scaled-up Kawai-cell," Phys. Earth Planet. Inter. **189**(1–2), 92–108 (2011).
[40]Shinmei, T., Irifune, T., Tsuchiya, J., and Funakoshi, K.-I., "Phase transition and compression behavior of phase D up to 46 GPa using multi-anvil apparatus with sintered diamond anvils," High Pressure Res. **28**(3), 363–373 (2008).
[41]Vaughan, M., Weidner, D. J., Wang, Y., Chen, J. H., Koleda, C. C., and Getting, I. C., "T-cup: A new high-pressure apparatus for X-ray studies," Rev. High Pressure Sci. Technol. **7**, 1520–1522 (1998).
[42]Walker, D., Carpenter, M. A., and Hitch, C. M., "Some simplifications to multianvil devices for high pressure experiments," Am. Mineral. **75**, 1020–1028 (1990).
[43]Walte, N., Rubie, D., Bons, P., and Frost, D., "Deformation of a crystalline aggregate with a small percentage of high-dihedral-angle liquid: Implications for core–mantle differentiation during planetary formation," Earth Planet. Sci. Lett. **305**(12), 124–134 (2011).
[44]Wang, Y., Durham, B., Getting, I. C., and Weidner, D. J., "The deformation-DIA: A new apparatus for high temperature triaxial deformation to pressures up to 15GPa," Rev. Sci. Instrum. **74**(6), 3002–3011 (2003).
[45]Weir, C. E., Lippincott, E. R., Van Valkenburg, A., and Bunting, E. N., "Infrared studies in the 1- to 15-micron region to 30,000 atmospheres," J. Res. Natl. Bur. Stand., Sect. A **63A**(1), 55 (1959).
[46]Yamazaki, D. and Karato, S.-i., "High-pressure rotational deformation apparatus to 15 GPa," Rev. Sci. Instrum. **72**(11), 4207–4211 (2001).